Multivariate Integer Cycle-Slip Resolution: A Single-Channel Analysis

P.J.G. Teunissen and P.F. de Bakker

Abstract

In this contribution we study the strength of the single-receiver, single-channel GNSS model for instantaneously resolving integer cycle-slips. This will be done for multi-frequency GPS, Galileo and BeiDou, thereby focusing on the challenging case that the slip is due to a simultaneous loss of lock on all frequencies. The analytical analysis presented is supported by means of numerical results.

Keywords

Global navigation satellite systems (GNSS) • Integer cycle-slip • Single-channel model

1 Introduction

Integrity monitoring and quality control can be exercised at different stages of the GNSS data processing chain. These stages range from the single-receiver, single-channel case to the multi-receiver/antenna case, sometimes even with additional constraints included.

In the present contribution, we consider the single-receiver, single-channel model. It is a challenging model as it is the weakest of all, due to the absence of the relative receiver-satellite geometry. In Teunissen and de Bakker (2012), we studied this model's multi-frequency GNSS integrity performance against modelling errors such as code outliers, carrier-phase slips and ionospheric disturbances. By means of the minimal detectable biases (MDBs) of the uniformly most powerful invariant (UMPI) test statistics, it was shown how well these modelling errors can be found.

In (ibid.) the carrier-phase slips were allowed to be non-integer, and therefore real-valued, as well. This implied that hypothesis testing theory with the DIA-method for the detection, identification and adaptation of the modelling error could be directly applied (Teunissen 1998a). In the present study, however, attention is restricted to *integer* slips only.

The problem of detecting and recovering from integer cycle-slips is an important one and one that has already been considered in several studies, see e.g. (Bisnath et al. 2001; Liu 2010; Carcanague 2012) for the dual-frequency case and (Dai et al. 2009; Xie et al. 2013) for the triple frequency case. It seems, however, that one is of two minds in these studies. On the one hand, namely in the detection step, one treats the slips as real-valued (i.e. integerness is not imposed), while on the other hand, after one has decided that a slip indeed occurred, one imposes the integerness by estimating it as such. This is not consistent and also not needed. Moreover, the cycle-slip detector used in these studies is often not an UMPI-test statistic.

In the present contribution we will not make the above referred to difference between *real-valued* slip-detection and *integer-valued* slip-repair. Instead we estimate the slip directly as an integer and use its probability mass function for evaluation. Consider the following slip-free and slip-biased models,

$$\begin{aligned} \mathscr{H}_0 &: \; \mathrm{E}(y) = Gx, \qquad\quad x \in \mathbb{R}^l, \; \mathrm{D}(y) = Q_{yy} \\ \mathscr{H}_a &: \; \mathrm{E}(y) = Gx + Hz, \; z \in \mathbb{Z}^n, \; \mathrm{D}(y) = Q_{yy} \end{aligned} \tag{1}$$

P.J.G. Teunissen (✉) • P.F. de Bakker
Department of Spatial Sciences, GNSS Research Centre, Curtin University of Technology, Perth, WA 6845, Australia

Department of Geoscience and Remote Sensing, Delft University of Technology, Delft, The Netherlands
e-mail: p.debakker@curtin.edu.au; p.teunissen@curtin.edu.au

International Association of Geodesy Symposia,
DOI 10.1007/1345_2015_69,

Table 1 GPS, Galileo, BeiDou frequencies (f) and wavelengths (λ), and zenith-referenced standard deviations of undifferenced code (p) and phase (ϕ) observables

Signal	L1	L2	L5	E1	E5a	E5b	E5	E6	B1	B3	B2
f (MHz)	1575.42	1227.60	1176.45	1575.42	1176.45	1207.14	1191.795	1278.75	1561.1	1268.52	1207.14
λ (cm)	19.0	24.4	25.5	19.0	25.5	24.8	25.2	23.4	19.2	23.63	24.83
p (cm)	25	25	15	20	15	15	7	15	31	25	30
ϕ (mm)	1.0	1.3	1.3	1.0	1.3	1.3	1.3	1.2	1.4	1.7	1.6

These results were aggregated for GIOVE-B from Simsky et al. (2008), for GPS+GIOVE A/B from de Bakker et al. (2012) and from initial BeiDou results obtained at Curtin's GNSS Research Centre (Khodabandeh and Odolinski, 2013, BeiDou standard deviations, "Personal communication")

with y normally distributed and z denoting the integer cycle-slip. Let $\hat{x}_0$ and $\check{x}_a$ be the least-squares estimators of x under $\mathscr{H}_0$ and $\mathscr{H}_a$, respectively. Then

$$\check{x}_a = \hat{x}_0 - G^+ H \check{z} \tag{2}$$

with $G^+ = (G^T Q_{yy}^{-1} G)^{-1} G^T Q_{yy}^{-1}$ the least-squares inverse of G and $\check{z}$ the integer least-squares estimator of z. In general the distribution of $\hat{x}_0$ under $\mathscr{H}_0$ will differ from that of $\check{x}_a$ under $\mathscr{H}_a$. The latter has namely the multi-modal distribution as given in Teunissen (1999a). However, in case the probability of correct integer estimation $\mathrm{P}(\check{z} = z)$, also known as success-rate, is sufficiently large, then the distribution of $\check{x}_a$ can be approximated by a normal distribution. In that case the distribution of $\check{x}_a$ under $\mathscr{H}_a$ can be considered given by the distribution of $\hat{x}_0$ under $\mathscr{H}_0$:

$$\check{x}_a|\mathscr{H}_a \sim \hat{x}_0|\mathscr{H}_0 \sim \mathrm{N}(x, Q_{\hat{x}_0\hat{x}_0}) \tag{3}$$

Thus if the success-rate is sufficiently large, the decision whether or not a slip occurred (the so-called detection) is automatically implied in the above correction (2): if the outcome of $\check{z}$ is zero, then $\mathscr{H}_0$ is considered true, otherwise it is assumed that a cycle slip is detected.

In this contribution we study the single-receiver, single-channel model's ability to achieve sufficiently high success-rates for the estimated integer cycle-slip vector. This will be done for multi-frequency GPS, Galileo and BeiDou, thereby focusing on the challenging case that the slip is due to a complete loss-of-lock, i.e. a loss of lock on all frequencies. The results show that instantaneous integer cycle-slip resolution is possible for multi-frequency Galileo, but for triple-frequency GPS and BeiDou only for cut-off elevation angles larger than 25°.

2 The n-Frequency, 1-Receiver, 2-Epoch Model

2.1 The Observation Equations

The carrier phase and pseudorange (code) observation equations of a single receiver that tracks a single satellite on frequency $f_j = c/\lambda_j$ (c is speed of light, λ_j is jth wavelength and $j = 1, \ldots, n$) at time instant t ($t = 1, \ldots, k$), are given as

$$\begin{aligned} \phi_j(t) &= \rho^*(t) - \mu_j i(t) + b_{\phi_j} + n_{\phi_j}(t) \\ p_j(t) &= \rho^*(t) + \mu_j i(t) + b_{p_j} + n_{p_j}(t) \end{aligned} \tag{4}$$

where $\phi_j(t)$ and $p_j(t)$ denote the single receiver observed carrier phase and pseudorange, respectively, with corresponding zero mean noise terms $n_{\phi_j}(t)$ and $n_{p_j}(t)$. The unknown parameters are $\rho^*(t)$, $i(t)$, b_{ϕ_j} and b_{p_j}. The lumped parameter $\rho^*(t) = \rho(t) + c\delta t_r(t) - c\delta t^s(t) + T(t)$ is formed from the receiver-satellite range $\rho(t)$, the receiver and satellite clock errors, $c\delta t_r(t)$ and $c\delta t^s(t)$, respectively, and the tropospheric delay $T(t)$. The parameter $i(t)$ denotes the ionospheric delay expressed in units of range with respect to the *first* frequency. Thus for the f_j-frequency pseudorange observable, its coefficient is given as $\mu_j = f_1^2/f_j^2$. The GPS, Galileo and BeiDou frequencies and wavelengths are given in Table 1. The parameters b_{ϕ_j} and b_{p_j} are the phase bias and the instrumental code delay, respectively. The phase bias is the sum of the initial phase, the phase ambiguity and the instrumental phase delay.

Both b_{ϕ_j} and b_{p_j} are assumed to be time-invariant. This is allowed for relatively short time spans, in which the instrumental delays remain sufficiently constant (Liu et al. 2004). The time-invariance of b_{ϕ_j} and b_{p_j} implies that only time-differences of $\rho^*(t)$ and $i(t)$ are estimable. We may therefore just as well formulate the observation equations in time-differenced form. Then the parameters b_{ϕ_j} and b_{p_j} get eliminated and we obtain

$$\begin{aligned} \phi_j(t,s) &= \rho^*(t,s) - \mu_j i(t,s) + n_{\phi_j}(t,s) \\ p_j(t,s) &= \rho^*(t,s) + \mu_j i(t,s) + n_{p_j}(t,s) \end{aligned} \tag{5}$$

where $\phi_j(t,s) = \phi_j(t) - \phi_j(s)$, with a similar notation for the time-difference of the other variates.

Would we have a priori information available about the ionospheric delays, we could model this through the use of additional observation equations. In our case, we do not assume information about the *absolute* ionospheric delays, but rather on the *relative*, time-differenced, ionospheric delays. We therefore have the (pseudo) observation equation

$$i_o(t,s) = i(t,s) + n_i(t,s) \tag{6}$$

with the (pseudo) ionospheric observable $i_o(t,s)$. The sample value of $i_o(t,s)$ is usually taken to be zero.

2.2 The Null- And Alternative Hypothesis

If we define $\phi(t,s) = (\phi_1(t,s),\ldots,\phi_n(t,s))^T$, $p(t,s) = (p_1(t,s),\ldots,p_n(t,s))^T$, $y = (\phi(t,s)^T, p(t,s)^T, i_o(t,s))^T$, $x = (\rho^*(t,s), i(t,s))^T$, then the n-frequency, 2-epoch model can be written in compact matrix-vector form as

$$\mathscr{H}_0: \quad \mathrm{E}(y) = Gx \;\;,\;\; \mathrm{D}(y) = Q_{yy} \;, y \in \mathbb{R}^{2n+1}, x \in \mathbb{R}^2 \tag{7}$$

where

$$G = \begin{bmatrix} e_n & -\mu \\ e_n & +\mu \\ 0 & 1 \end{bmatrix} \;\;,\;\; Q_{yy} = \mathrm{blockdiag}(2Q_{\phi\phi}, 2Q_{pp}, \sigma_{di}^2) \tag{8}$$

with e_n the n-vector of ones, $\mu = (\mu_1,\ldots,\mu_n)^T$, $Q_{\phi\phi}$ and Q_{pp} the $n \times n$ variance matrices of the undifferenced phase and code observables, and scalar σ_{di}^2 the variance of the time-differenced ionospheric delay.

In our computations we assumed the variance matrices $Q_{\phi\phi}$ and Q_{pp} to be diagonal with its entries derived from Table 1. Since these entries are zenith-referenced, they still need to be multiplied with an elevation dependent factor to account for the elevation dependency. Based on the customary elevation-dependent models (Euler and Goad 1991), we used the following factors: 1.5 for 30°–40°, 2 for 25°–30°, and 3 for 15°–20° elevation range.

If we assume that the time series of the ionospheric delays can be modeled as a *first-order autoregressive* stochastic process, then

$$\sigma_{di}^2 = 2\sigma_i^2(1-\beta^{|t-s|}) \tag{9}$$

For two successive epochs we have $\sigma_{di}^2 = 2\sigma_i^2(1-\beta)$, while for larger time-differences the variance will tend to the white-noise value $\sigma_{di}^2 = 2\sigma_i^2$ if $\beta < 1$. Thus σ_i^2 and β can be used to model the level and smoothness of the noise in the ionospheric delays. We determined the approximate range of σ_{di}-values as given in Table 2.

Model (7) will be referred to as our null hypothesis $\mathscr{H}_0$. This null-hypothesis assumes that no loss-of-lock occurred between the two epochs. Would such loss-of-lock occur, however, then one or more of the n carrier-phases may become biased by an unknown number of integer cycle slips. Here we assume the worst scenario, namely that all n of the carrier-phases are affected by the loss-of-lock. Hence, instead of a one-dimensional integer cycle-slip, we consider the case of an integer cycle-slip vector $z \in \mathbb{Z}^n$. The model

Table 2 Approximate range of values for σ_{di} (m) when sampling with intervals of 1, 10 and 30 s, respectively, using a 10 degree cut-off elevation angle

	min. σ_{di}	max. σ_{di}
1 s	1.5×10^{-3}	3×10^{-3}
10 s	2×10^{-3}	10^{-2}
30 s	4.5×10^{-3}	2.5×10^{-2}

These values were obtained for mid-latitude (Delft) under moderate ionospheric conditions

for such 'loss-of-lock' hypothesis is given by the alternative hypothesis

$$\mathscr{H}_a: \; \mathrm{E}(y) = [G, H]\begin{bmatrix} x \\ z \end{bmatrix} \;,\; \mathrm{D}(y) = Q_{yy} \;,\; z \in \mathbb{Z}^n \tag{10}$$

with $H = [\Lambda, 0, 0]^T$ and $\Lambda = \mathrm{diag}[\lambda_1,\ldots,\lambda_n]$.

3 Estimability of Multivariate Carrier-Phase Slip

3.1 Variance Matrix of Multivariate Cycle-Slip Estimator

From the structure of $[G, H]$ in (10), it follows that the carrier phase vector $\phi(t,s)$ will not contribute to the estimation of the parameters $\rho^*(t,s)$ and $i(t,s)$ under $\mathscr{H}_a$. These parameters are therefore solely determined by the code observables and a priori ionospheric information. As a consequence, the two-epoch cycle-slip estimator is given as the difference $\hat{z} = \Lambda^{-1}(\phi(t,s) - \hat{\phi}(t,s))$, where $\hat{\phi}(t,s) = e_n\hat{\rho}^*(t,s) - \mu\hat{i}(t,s)$ is the least-squares phase estimator based solely on the code observables and a priori ionospheric information. Solving for $\hat{\rho}^*(t,s)$ and $\hat{i}(t,s)$, followed by applying the variance propagation law to $\hat{z} = \Lambda^{-1}(\phi(t,s) - e_n\hat{\rho}^*(t,s) + \mu\hat{i}(t,s))$ gives then the variance matrix of the multivariate cycle-slip estimator. The result is given in the following Lemma.

Lemma 1 (Variance Matrix Multivariate Slip) *The variance matrix of the least-squares estimator of z under $\mathscr{H}_a$ is given as*

$$Q_{\hat{z}\hat{z}} = \Lambda^{-1}\left(\underbrace{2Q_{\phi\phi}}_{\text{phase}} + \underbrace{2P_{e_n}Q_{pp}P_{e_n}^T}_{\text{code;rank=1}} + \underbrace{(R_{e_n}\mu)\sigma_{d\hat{i}}^2(R_{e_n}\mu)^T}_{\text{ionosphere;rank=1}}\right)\Lambda^{-1} \tag{11}$$

with $R_{e_n} = I_n + P_{e_n}$, $P_{e_n} = e_n(e_n^T Q_{pp}^{-1} e_n)^{-1} e_n^T Q_{pp}^{-1}$, $P_{e_n}^{\perp} = I_n - P_{e_n}$, *and where*

$$\sigma^2_{d\hat{i}} = \frac{\sigma^2_{di}}{1 + \frac{1}{2}\sigma^2_{di} \underbrace{||\mu - \bar{\mu}_p||^2_{Q_{pp}}}_{\text{frequency-diversity}}} \quad , \quad \bar{\mu}_p = P_{e_n}\mu \qquad (12)$$

◇

Note that the slip variance matrix is a sum of three terms, the entries of which may differ substantially in size. The first matrix term in this sum is governed by the precision of the phase observables and will therefore have small entries. The second matrix term is governed by the precision of the code observables and will therefore have generally much larger entries than the first matrix term in the sum. The third matrix term depends, next to the precision of the code observables, also on μ and σ^2_{di}. Its entries will become smaller, if $\sigma^2_{d\hat{i}}$ gets smaller. This happens for smaller σ^2_{di} (smoother ionospheric delays) and/or larger $||\mu - \bar{\mu}_p||^2_{Q_{pp}}$ (better code precision and/or larger frequency diversity). Thus if $\sigma^2_{di} = \infty$, frequency diversity is needed (i.e. $||\mu - \bar{\mu}_p||^2_{Q_{pp}} \neq 0$) so as to avoid the entries of the third matrix term in (11) to become infinite.

Due to the relative poor code precision (as compared to phase) the confidence ellipsoid of $\hat{z}$ is usually very elongated. This elongation gets larger if σ_{di} gets larger. Figure 1 shows the dual-frequency L1/L2 confidence ellipse of the cycle-slip estimator $\hat{z}$ for different values of the ionospheric standard deviation. Such an elongated ellipse implies that the component of the cycle-slip in the direction of elongation is poorly estimable, whereas the component orthogonal to it, is very well estimable. Note that for larger σ_{di}, the elongation approximately points into the $z_1 = z_2$-direction. This explains why in those cases the wide-lane combination has good precision. But also note, that the ellipse rotates away from the $z_1 = z_2$-direction as σ_{di} gets smaller. This implies that for those cases other combinations than the wide-lane have better precision.

If we consider more than $n = 2$ frequencies, it is important to point out that the second and third matrix terms of (11) are both of rank 1. This implies that the elongation of the confidence ellipsoid of $\hat{z}$ remains restricted to two dimensions only, irrespective the value of $n \geq 2$. This indicates that in higher dimensions one should be able to profit from the increase in frequencies and thus better be able to successfully resolve the integer cycle-slip vector in case of a loss-of-lock. To what extent this is possible, will be investigated further in the next sections.

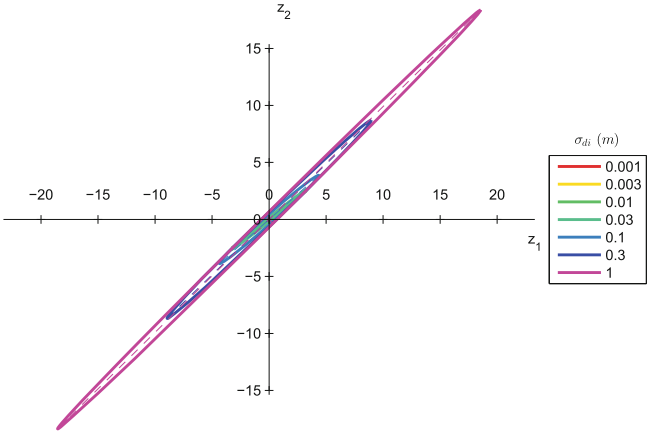

Fig. 1 Dual-frequency L1/L2, 95% confidence ellipse of cycle-slip estimator $\hat{z}$, for different values of ionospheric standard deviation σ_{di} (cf. 11). Units along axes are cycles

4 The ADOP of the Multivariate Slip

The ADOP was introduced in Teunissen (1997) as an easy-to-compute scalar diagnostic to measure the *intrinsic* model strength for successful ambiguity resolution. The ADOP is defined as the square-root of the ambiguity variance matrix determinant taken to the power one over the number of integer ambiguities, which, in the present case, is the dimension of the integer cycle-slip vector z,

$$\text{ADOP} = |Q_{\hat{z}\hat{z}}|^{\frac{1}{2n}} \quad \text{(cycle)} \qquad (13)$$

The ADOP has the important property that it is invariant against the choice of ambiguity parametrization. Since all admissible ambiguity transformations can be shown to have a determinant of ± 1, the ADOP does not change when one changes the definition of the ambiguities. It therefore measures the intrinsic precision of the ambiguities. As a rule-of-thumb, an ADOP smaller than about 0.10 cycle, corresponds to an ambiguity success-rate larger than 0.999.

From the variance matrix of Lemma 1, an analytical closed-form formula can be derived for the corresponding ADOP. A useful and easy-to-interpret approximation to this analytical expression is given in the following lemma.

Lemma 2 (ADOP Rule-of-Thumb) *If* $Q_{\phi\phi} = \sigma^2_{\phi} I_n$ *and* $Q_{pp} = \sigma^2_p I_n$, *then the ambiguity dilution of precision of the multivariate cycle-slip can be approximated as*

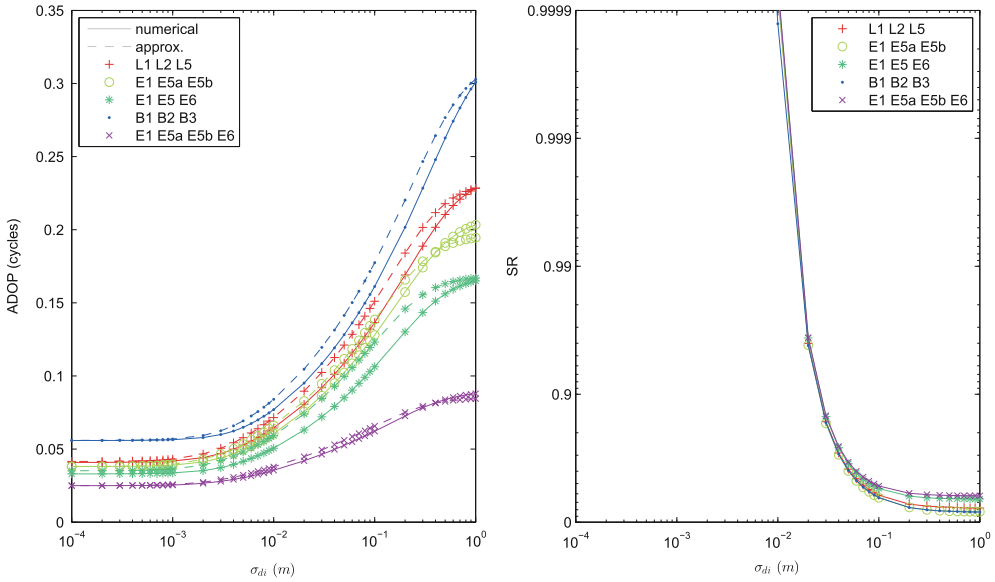

Fig. 2 *Left*: Multi-frequency cycle-slip ADOPs, as function of σ_{di}, for GPS, Galileo and BeiDou. The *dashed curves* are based on the approximation (14), while the *full curves* are based on (13); *Right*: Multi-frequency, zenith-referenced, bootstrapped success-rates (SR) of resolving the integer cycle-slip vector z, as function of σ_{di}, for GPS, Galileo and BeiDou

$$\text{ADOP} \approx \left(\frac{\sqrt{2}}{\bar{\lambda}}\right)\left[\alpha \underbrace{\left(\sigma_\phi^{n-1}\sigma_p\right)^2}_{\text{iono-fixed}} + (1-\alpha)\underbrace{\left(\sigma_\phi^{n-2}\sigma_p^2\right)^2}_{\text{iono-float}}\right]^{\frac{1}{2n}} \tag{14}$$

with $\bar{\lambda} = \prod_{i=1}^n \lambda_i^{\frac{1}{n}}$ *and* $\alpha = [1+\frac{1}{2}\sum_{i=1}^n(\mu_i-\bar{\mu})^2\sigma_{di}^2/\sigma_p^2]^{-1}$. ◇

Note that $\bar{\lambda}$ is the geometric average of the wavelengths, whereas $\bar{\mu}$ is the arithmetic average of the μ_i. Also note that the term within the square brackets is a *convex* combination driven by the scalar α. For $\alpha = 1$, the ionosphere-fixed result is obtained, while for $\alpha = 0$ the ionosphere-float result is obtained. Thus

$$\begin{aligned}\text{ADOP}_{\alpha=1} &\approx \left(\tfrac{\sqrt{2}}{\bar{\lambda}}\right)\left(\sigma_\phi^{n-1}\sigma_p\right)^{\frac{1}{n}} \qquad (\text{iono}-\text{fixed})\\ \text{ADOP}_{\alpha=0} &\approx \left(\tfrac{\sqrt{2}}{\bar{\lambda}}\right)\left(\sigma_\phi^{n-2}\sigma_p^2\right)^{\frac{1}{n}} \qquad (\text{iono}-\text{float})\end{aligned} \tag{15}$$

This clearly shows the roles played by the contributing factors: wavelengths ($\bar{\lambda}$), phase precision (σ_ϕ), code precision (σ_p) and number of frequencies (n). It also shows the very different contributions of phase and code to either the ionosphere-fixed case or the ionosphere-float case. For instance, for the single-frequency case, $n = 1$, the ionosphere-fixed ADOP is driven by the code-precision only, whereas for the ionosphere-float case, the ADOP gets further magnified by σ_p/σ_ϕ, i.e. a factor of about 100. For an arbitrary number of frequencies the ratio between the two ADOPs is given as

$$\frac{\text{ADOP}_{\alpha=1}}{\text{ADOP}_{\alpha=0}} \approx \left(\frac{\sigma_\phi}{\sigma_p}\right)^{\frac{1}{n}} \tag{16}$$

Figure 2(Left) shows, as function of σ_{di}, the multi-frequency, loss-of-lock cycle-slip ADOPs for GPS, Galileo and BeiDou. These results are promising as the ADOPs are all below 0.1 cycle for most of the relevant σ_{di}-range (cf. Table 2). In the next section we will study their success-rates.

5 Multi-Frequency, Cycle-Slip Resolution Success-Rates

5.1 Bootstrapped Success-Rates

Different integer estimators can be used to solve for the integer cycle-slip vector z. Three popular integer estimators are integer rounding, integer bootstrapping and integer least-squares. As the following theorem shows, there exists a clear ordering among these three estimators.

Theorem 1 (Teunissen 1999b) *Let* $\hat{z} \sim \text{N}(z, Q_{\hat{z}\hat{z}})$ *and let* $\check{z}_{\text{IR}}$, $\check{z}_{\text{IB}}$, *and* $\check{z}_{\text{ILS}}$ *denote the estimators of integer rounding, integer bootstrapping and integer least-squares, respectively. Then their success-rates are ordered as*

$$\text{P}(\check{z}_{\text{IR}} = z) \le \text{P}(\check{z}_{\text{IB}} = z) \le \text{P}(\check{z}_{\text{ILS}} = z) \tag{17}$$

◇

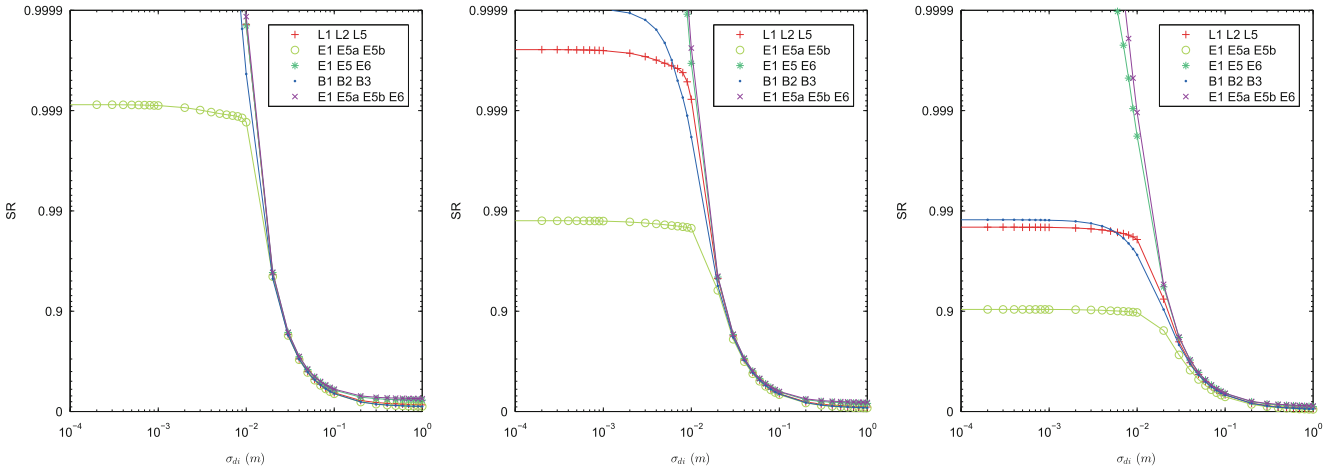

Fig. 3 Multi-frequency, GPS, Galileo and BeiDou, bootstrapped success-rates (SR) of resolving the integer cycle-slip vector z, as function of σ_{di}, for different elevation angles (*Left*: 30°–40°, *Middle*: 25°–30°, *Right*: 15°–20°)

Integer rounding (IR) is the simplest, but it also has the poorest success rate. Integer least-squares (ILS) is the most complex, but also has the highest success rate of all. Integer bootstrapping (IB) sits in between. It does not need an integer search as is the case with ILS, and it does not completely neglect the information content of the ambiguity variance matrix as IR does. Moreover, bootstrapping is the only integer estimator for which an easy-to-use and exact expression can be given of its success-rate. This success-rate is given in the following theorem.

Theorem 2 (Teunissen 1998b) *Let* $\hat{z} \sim \mathrm{N}(z, Q_{\hat{z}\hat{z}})$. *Then the success-rate of integer bootstrapping is given as*

$$\mathrm{P}(\check{z}_{\mathrm{IB}} = z) = \prod_{i=1}^{n} \left(2\Phi\left(\frac{1}{2\sigma_{z_i|I}} \right) - 1 \right) \qquad (18)$$

with $\Phi(x) = \int_{-\infty}^{x} \frac{1}{\sqrt{2\pi}} \exp\{-\frac{1}{2}v^2\} dv$ *and* $\sigma_{z_i|I}$ *the standard deviation of the* i*th entry of* $\hat{z}$, *conditioned on the previous* $I = \{1, \ldots, (i-1)\}$ *entries.* $\diamond$

In this contribution we used the bootstrapped success-rate. It has been used after applying the decorrelating transformation of the LAMBDA method (Teunissen 1995a). For such decorrelated cases namely, the bootstrapped success-rate becomes a sharp lower bound of the ILS success-rate.

Figure 2(Right) shows the cycle-slip vector resolution success-rates for the same frequency-combinations as shown in Fig. 2(Left). As predicted by the ADOPs, the success-rates are indeed very high, 99.99% or larger for $\sigma_{di} \leq 10^{-2}$. However, the results of Fig. 2(Left and Right) are zenith-referenced and therefore only hold true for an elevation angle of 90°.

5.2 Success-Rates Versus Elevation

For the same frequency combinations as before, Fig. 3 now shows the success-rates for different elevation angles. The results clearly show that the success-rates get smaller as the elevation angle gets smaller. The results also show that some frequency combinations are more sensitive than others to the changes in elevation angle. For instance, the success-rate of the Galileo frequency combination E1-E5a-E5b, is the first to drop in value when the elevation gets smaller, see Fig. 3(Left). The combinations that retain a large success-rate, even at low elevation, are the triple and quadruple Galileo combinations E1-E5-E6 and E1-E5a-E5b-E6, see Fig. 3(Right). For these combinations one can expect to have at least a 99.9% success-rate up to $\sigma_{di} = 10^{-2}$ m.

Also note, although the triple-frequency success-rates of GPS and BeiDou are too low for low elevations, their success-rates are still large for elevations in the 25°–30° range, see Fig. 3(Middle). This is a relevant finding, since as shown in Odolinski et al. (2013a), positioning with a combined GPS and BeiDou system will allow one to make use of much higher cut-off elevation angles. Similarly, it was shown in Nadarajah and Teunissen (2013) that this is true for GPS+BeiDou MC-LAMBDA attitude determination as well. Hence, for those positioning and attitude-determination applications, instantaneous loss-of-lock integer cycle slip resolution will become feasible.

References

Bisnath SB, Kim D, Langley RB (2001) Carrier Phase Slips: a new approach to an old problem. GPS World, 12(5), 46–51

Carcanague S (2012) Real-time geometry-based cycle slip resolution technique for single-frequency PPP and RTK. In: Proceedings of the 25th ITM, pp 1136–1148

Dai Z, Knedlik S, Loffeld O (2009) Instantaneous triple-frequency GPS cycle-slip detection and repair. Int J Navig Obs p 15. Doi:10.1155/2009/407231

de Bakker PF, Tiberius CCJM, van der Marel H, van Bree RJP (2012) Short and zero baseline analysis of GPS L1 C/A, L5Q, GIOVE E1B, and E5aQ signals. GPS Solutions, 16, 53–64

Euler H-J, Goad CC (1991) On optimal filtering of GPS dual frequency observations without using orbit information. Bull Géod 65:130–143

Liu Z (2010) A new automated cycle-slip detection and repair method for a single dual-frequency GPS receiver. J Geod. Doi:10.1007/s00190-010-0426-y

Liu X, Tiberius CCJM, de Jong K (2004) Modelling of differential single difference receiver clock bias for precise positioning. GPS Solution 4:209–221

Nadarajah N, Teunissen PJG (2013) Instantaneous GPS/BeiDou/Galileo attitude determination: a single-frequency robustness analysis under constrained environments. In: Proceedings of the institute of navigation pacific PNT 2013, pp 1088–1103

Odolinski R, Teunissen PJG, Odijk D (2013a) An analysis of combined COMPASS/BeiDou-2 and GPS single- and multiple-frequency RTK positioning. In: Proceedings of the institute of navigation pacific PNT 2013, pp 69–90

Simsky A, Mertens D, Sleewaegen J-M, De Wilde W, Hollreiser M, Crisci M (2008) MBOC vs. BOC(1,1) mulipath comparison based on GIOVE-B data. Inside GNSS, September/October, pp 36–39

Teunissen PJG (1995a) The least-squares ambiguity decorrelation adjustment: a method for fast GPS integer ambiguity estimation. J Geod 70:65–82

Teunissen PJG (1997) A canonical theory for short GPS baselines. Part IV: precision versus reliability. J Geod 71:513–525

Teunissen PJG (1998a) Minimal detectable biases of GPS data. J Geod 72:236–244

Teunissen PJG (1998b) Success probability of integer GPS ambiguity rounding and bootstrapping. J Geod 72:606–612

Teunissen PJG (1999a) The probability distribution of the GPS baseline for a class of integer ambiguity estimators. J Geod 73:275–284

Teunissen PJG (1999b) An optimality property of the integer least-squares estimator. J Geod 73:587–593

Teunissen PJG, de Bakker PF (2012) Single-receiver single-channel multi-frequency GNSS integrity: outliers, slips, and ionospheric disturbances. J Geod Doi: 10.1007/s00190-012-0588-x

Xie K, Chai H, Wang M, Pan Z (2013) Cycle slip detection and repair with different sampling interval based on compass triple-frequency. In: Sun J, et al (eds) Proceedings of China Satellite Navigation Conference (CSNC) 2013, pp 291–303